The Journal of Physical Chemistry Letters

A General Method to Determine the Flux of Charged Molecules Through Nanopores Applied to ß-Lactamase Inhibitors and OmpF

Journal:	*The Journal of Physical Chemistry Letters*
Manuscript ID	jz-2017-00062p
Manuscript Type:	Letter
Date Submitted by the Author:	10-Jan-2017

Complete List of Authors:	Ghai, Ishan; Jacobs-UNiversity Bremen, Life-Science Pira, Alessandro; Universita degli Studi di Cagliari, Dipartmento di Fisica Scorciapino, Mariano; Universita degli Studi di Cagliari, Dipartmento di Fisica Bodrenko, Igor; University of Cagliari, Department of Physics Benier, Lorraine; Jacobs-UNiversity Bremen, Life-Science Ceccarelli, Matteo; Universita degli Studi di Cagliari, Dipartmento di Fisica Winterhalter, Mathias; Jacobs University Bremen, School of Engineering and Science Wagner, Richard; Jacobs-UNiversity Bremen, Life-Science

A general method to determine the flux of charged molecules through nanopores applied to ß-lactamase inhibitors and OmpF

Subtitle: Permeation of ß-lactamase inhibitors through OmpF

Ishan Ghai,[1] Alessandro Pira,[2] Mariano Andrea Scorciapino,[3] Igor. Bodrenko,[2] Lorraine Benier,[1] Matteo Ceccarelli,[2] Mathias Winterhalter,[1] Richard Wagner[1]*

[1]Department of Life Sciences and Chemistry, Jacobs University Bremen, 28719 Bremen, Germany

[2]Department of Physics, University of Cagliari, Cagliari, Italy.

[3]Department of Biomedical Sciences, University of Cagliari, Cagliari, Italy.

*Corresponding author E-mail: ri.wagner@jacobs-university.de

Abstract: A major challenge in the discovery of the new antibiotics against Gram-negative bacteria is to achieve sufficiently fast permeation in order to avoid high doses causing toxic side effects. So far, suitable assays for quantifying the uptake of charged antibiotics into bacteria are lacking. We apply electrophysiological zero-current assays using concentration gradients of ß-lactamase-inhibitors combined with single channel condutance to quantfy their flux rates trough OmpF. Molecular dynamic simulations provide in addition details on the interactions between the nanopore wall and the charged solutes. In particular, the interaction barrier for three ß lactamase inhibitors is surprisingly as low as 3-5 kcal/mol, and only slightly above the diffusion barrier of ions such as chloride. Within our macroscopic constant field model, we determine that at zero-membrane potential a concentration gradient of 10 µM of avibactam, sulbactam or tazobactam can create a flux rates of roughly 620 molecules/s and per OmpF trimer.

Keywords: Translocation, Electrophoretic Mobilities, Reversal Potential, Molecular dynamics, Avibactam, Bacterial porins

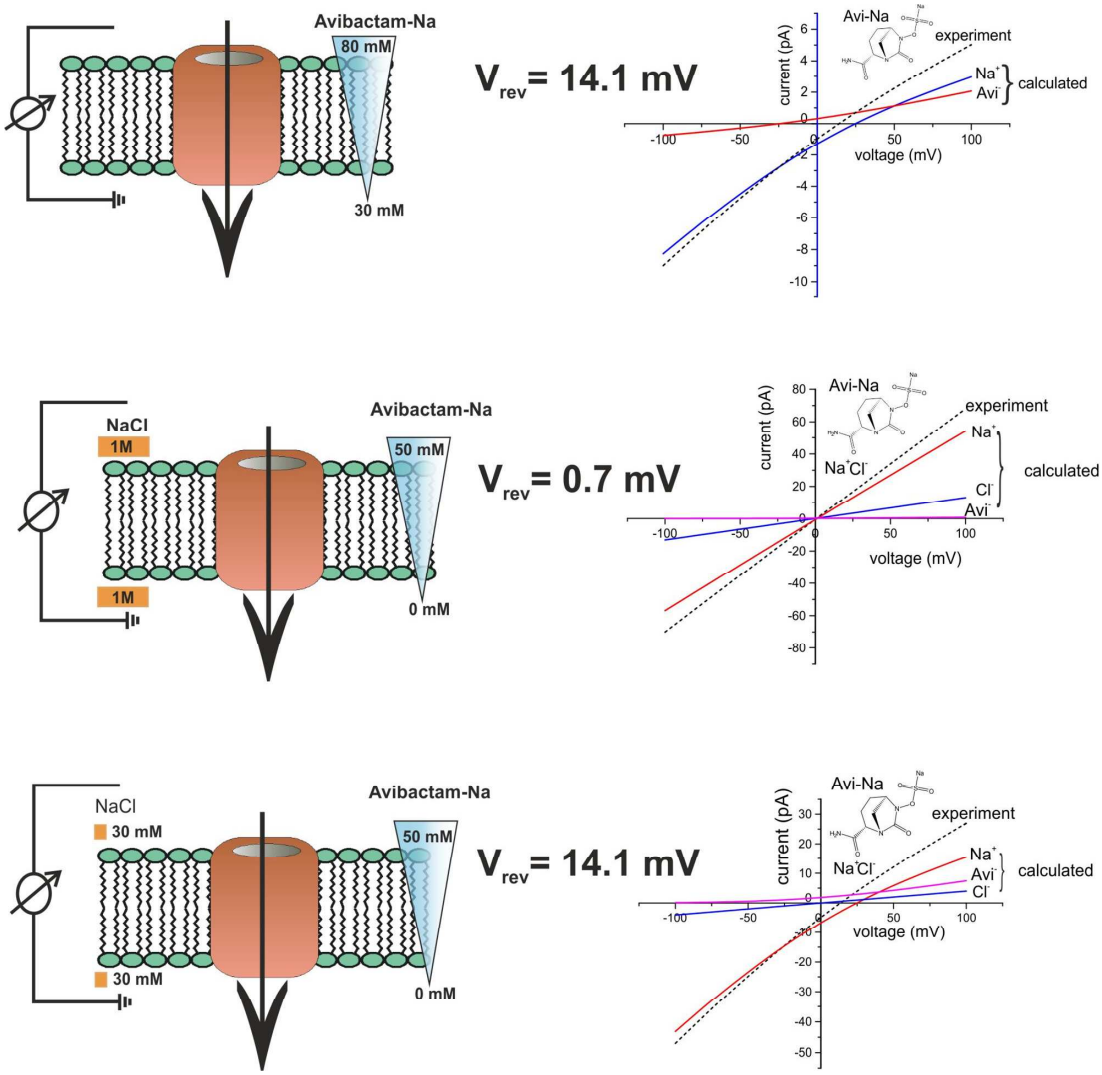
Avibactam-Na
80 mM
30 mM
V_{rev}= 14.1 mV
Avi-Na
experiment
Na+
Avi-
calculated
current (pA)
voltage (mV)
NaCl
1M
Avibactam-Na
50 mM
0 mM
V_{rev}= 0.7 mV
Na+Cl-
Cl-
NaCl
30 mM
Avibactam-Na
50 mM
0 mM
V_{rev}= 14.1 mV

Sensing of individual molecules has become an important analytical tool for biochemistry, biophysics, and chemistry, leading to development of next-generation bioanalytical and diagnostic tools.[1-2] Among single-molecule techniques, sensing with nanopores is a fast growing field with its most prominent application of high-throughput sensing of nucleic acids.[3-4] In nanopore sensing, individual molecules pass through a nanoscale pore thereby producing detectable changes in ionic currents[5].

Gram-negative bacteria have a complex cell envelope comprising an outer and an inner membrane that delimit the periplasm from the extracellular environment. The outer membrane contains numerous protein channels, called porins. These nanopores facilitate the chemical potential driven flux of small hydrophilic substances.[6] Porins are considered to be the main entry pathway for polar antibiotics, such as cephalosporins, penicillins, carbapenems and fluoroquinolones, as well as for charged ß-lactamase inhibitors.

In order to design the next generation of antibiotic molecules that will be able to overcome the membrane barrier more effectively, it is desirable to quantify the flux of individual solutes through nanopores present in the barrier.[6-7] Currently, the lack of such an assay is a substantial bottleneck for optimization of new molecules with respect to permeability and, ultimately, their antimicrobial activity against intact bacterial cells.[8] In order to support the urgent search for new antibiotics the European Union and the EFPIA financed the "New Drugs Against Bad Bugs" platform (www.ND4BB.eu). Within this platform "*Translocation"* is devoted to understand the low permeability problem.

Recently, we investigated the permeation of antibiotics through channels by analyzing the ion current fluctuations induced in the presence of substrates expected to permeate. Unfortunately, most small antimicrobial molecules do not produce easily detectable changes in the ion currents while passing the nanopore and require sophisticated extended current event or current noise analysis methods.[5,21] Here we present an approach to characterize transport of charged molecules even if they do not produce detectable changes in the nanopore current fluctuations.

To measure selectivity is a fast tool to obtain relative permeabilities between the ions present in solution. However, in order to determine turnover numbers additionally single channel conductances are requirred.[9-11] Here we describe an approach to quantify the permeation of three charged ß-lactamase inhibitors, namely, avibactam, sulbactam and tazobactam (Figure S1), through the OmpF porin from *Escherichia coli*. Moreover, we show that the macroscopic turnover number obtained experimentally can be complemented with all-atom molecular dynamics (MD) modeling, providing

atomic details on the selectivity, the energetics of transport and the correlated behavior of the ions. Our results show that the OmpF nanopore is highly permeable for the ß-lactamase inhibitors we have investigated. MD simulations reveal how these inhibitors find favorable interactions along a series of cationic residues inside the pore, just above the constriction region, with a rather low barrier to penetrate, between 3 and 5 kcal/mol, without blocking the channel to the passage of ions.

Results

Single channel recording under symmetric condition: bi and tri-ionic potential

In order to obtain information on permeation of ß-lactamase inhibitors through OmpF, we reconstituted trimeric OmpF into a planar lipid bilayer. In a 100 mM NaCl, 20 mM MES pH 6 buffer the channel revealed a conductance of $G_{trimer} = 960 \pm 100\, pS$ for the trimeric channel unit in agreement with previous publications (see supplemental information Figure S4 A, B).[12-13] Titration with Na-avibactam, Na-sulbactam and Na-tazobactam on both sides of the channel did not cause any significant concentration-dependent changes in channel gating (Figure S4 A) and thus no conclusion on the mode of possible transport could be drawn (see supplement for details) from this type of experiments.

In the second series of experiments, we measured OmpF conductance under symmetrical bi-ionic conditions, by using the sodium salts of the ß-lactamase inhibitors. Surprisingly replacing the chloride ion by the ß-lactamase inhibitors did change the conductance within the experimental error. (Table 1).

	Inhibitor/salt 30mM (cis/trans)	$\bar{G}_{trimer}$ **(pS) trimer**
OmpF	Avibactam-Na	270 pS ± 60 (n=15)
	Sulbactam-Na	240 pS ± 40 (n=27)
	Tazobactam-Na	240 pS ± 50 (n=36)
	NaCl	270 ± 60 (n=40)
OmpF Simulations	NaCl	190± 30 (n=4x200ns)

Table 1: Experimental and calculated conductance of an OmpF-trimer at low ionic strength under bi-ionic conditions. V=100 mV and 200 mV respectively for experiments and MD modeling.

Single channel recording under asymmetric condition: bi and tri-ionic potential

In order to gain information on the permeability of OmpF for the anionic ß-lactamase inhibitors, we applied an alternative experimental approach based on the Goldman-Hodgkin-Katz (GHK) current equation.[9] We followed a previous suggestion to analyze the selectivity of the OmpF containing artificial bilayer membranes under bi- and tri-ionic conditions on both sites of the planar bilayer.[10-11] Since ion fluxes are also created by concentration gradients the GHK current equation allows calculation of the relative ion permeability in a basic macroscopic model, using the chemical potential created by the different electrophoretic mobility of the ions themselves.[9] Starting from the GHK current equation for a given composition of ions in solution, the voltage dependent total ion current *I(V)* crossing a membrane channel is given by the sum of the individual ion currents $I_x(V)$[9].

(1) $$I(V) = \sum I_x(V)$$

and specifically in our case the main contributors are Na^+, Cl^- and the inhibitor (inh^-)

$$\sum I(V) = I_{Na^+}(V) + I_{Cl^-}(V) + I_{inh^-}(V)$$

with

(2) $$I_x(V, P_X, z, c_{cis}, c_{trans}) = P_x z^2 \frac{VF^2}{RT} \cdot \frac{\left(c_{x,cis} - c_{x,trans} exp\left(\frac{-zFV}{RT}\right)\right)}{1 - exp\left(\frac{-zFV}{RT}\right)}$$

where *V* is the transmembrane voltage, P_x the permeability for the ion x, z the valency, F = 9.6 10^4 As mol^{-1} the Faraday constant and R = 8.3 J mol^{-1} K^{-1} the gas constant. In the experimental input, $c_{x,cis}$ and $c_{x,trans}$ are the ion concentration on the two sites of the membrane, respectively.

In the experiments described below, the total current *I(V)* was measured at particular bi or tri-ionic conditions in the cis and trans compartment separated by a OmpF containing bilayer as a function of transmembrane voltages applied. With respect to antibiotics, it is worth mentioning that the typically poor solubility (in the order of few mM) is often a challenge, especially when this is combined with the availability of only small amounts, as antibiotics typically come from small scale synthesis of non-commercial products. To circumvent this issue, we applied an experimental setup where, starting from a symmetrical condition of low salt concentration on both sides of the membrane containing OmpF channels was supplemented with low concentration of the Na^+ salt of ß-lactamase inhibitor only on one side (tri-ionic conditions) to experimentally resolve single channel currents (see Supplemental Information for details). In addition, for calibration purpose we employed also asymmetric bi-ionic conditions by using the sodium salts of the ß-lactamase inhibitors on both sides of the membrane containing OmpF channels. Measurements of the current *vs* voltage (I-V) curves

with different ß-lactamase inhibitors under both bi- and tri-ionic conditions were performed as described in the Supplemental Information. Representative I-V plots are shown in Figure 1.

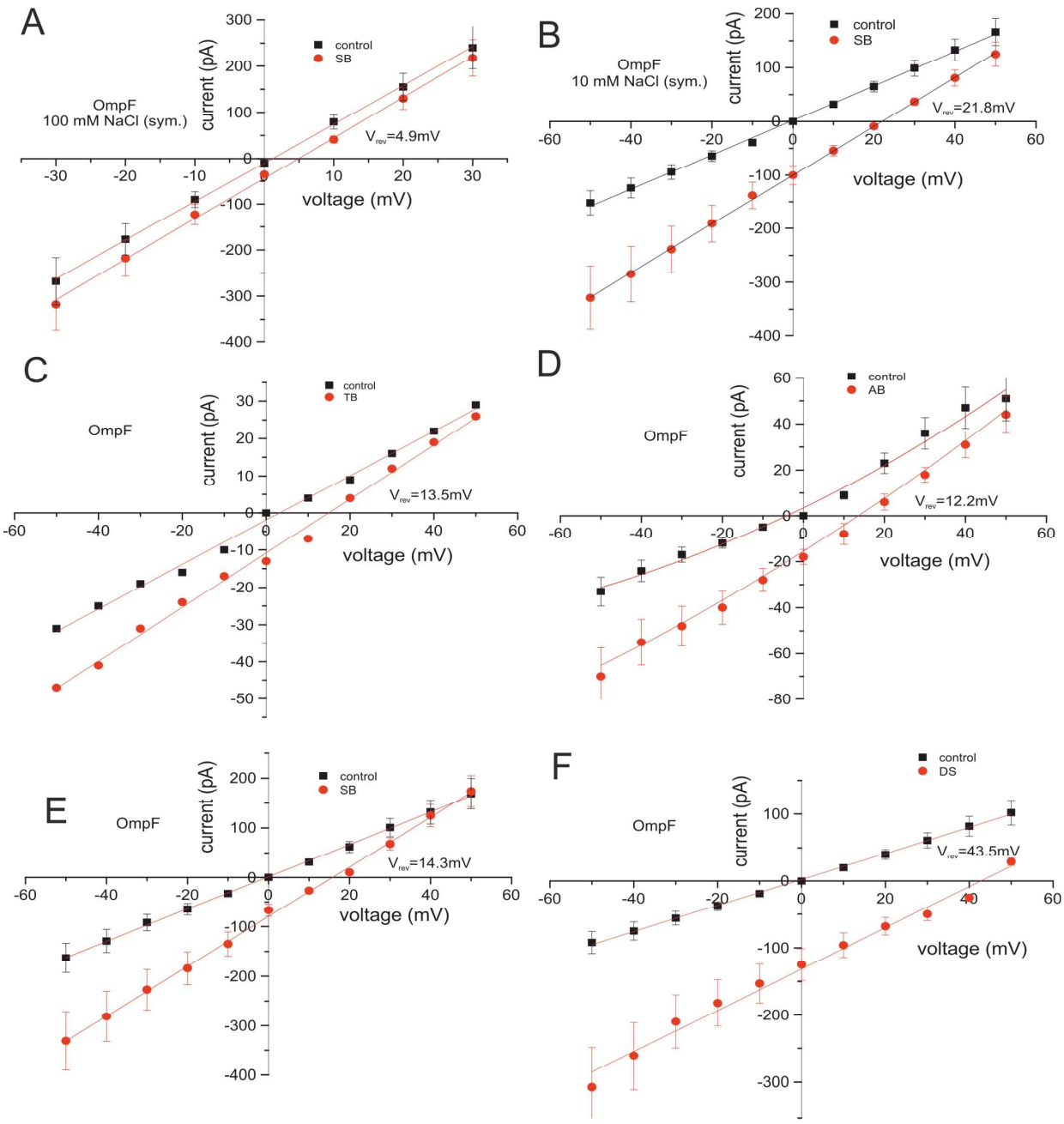

Figure 1: Selected I-V curves from bilayers containing one or many reconstituted OmpF channels with different ß-lactamase inhibitors under bi- and tri-ionic conditions. The cis side refers to the electrical ground. (A) Symmetrical 100 mM NaCl (cis/trans) in the absence (control) and presence

of additional 50 mM Na-sulbactam (cis); about 17 channels. (B) Symmetrical 10 mM NaCl (cis/trans) and additional 50mM Na-sulbactam (cis); 55 channels. (C) Bi-ionic recordings with symmetrical 30 mM Na-tazobactam (cis/trans) as control, and additional 50 mM Na-tazobactam on cis (80/30 mM Na-tazobactam cis/trans); 2 channels. (D) Same as (C) with Na-avibactam; 3 channels. (E) Same as (C) and (D) with Na-sulbactam; 8 channels. (F) Control measurement Bi-ionic recordings with symmetrical 10 mM Na-dextran sulfate (cis/trans) as control, and additional 50 mM Na-dextran sulfate on cis (60/10 mM Na-dextran sulfate cis/trans). Note that ion concentration values refer to the monomer of poly dextran and that each monomer sulfate group carries 3 Na^+, thus, additional 30 mM Na^+ (see Supplemental Information).

The different slopes of the I-V curves shown in Figure1 are due to a different number of channels incorporated into the respective bilayers. Nevertheless, reversal potentials are independent of the number of channels. Except for Na-dextran-sulfate (see below) all determined V_{rev} clearly show that the different ß-lactamase anions can pass the OmpF pore to a remarkable extend. The corresponding permeability ratios P_{inh^-}/P_{Na^+} were calculated as described in detail in the Supplemental Information. As a negative control, we used the Na^+-salt of the large branched polysaccharide, poly-dextran sulfate ($average\ \overline{Mw} \cong$ 8kDa, r_{Stokes}>2.5nm), since the large anion is expected not to permeate the OmpF pore (Figure 1F) With a Na-dextran-sulfate gradient of (60/10 mM, cis/trans) we obtained V_{rev} = 43 ± 3.4 mV. This value of V_{rev} is within experimental error identical to the Nernst potential (defined as the potential which appears if only one type of ion permeates) of $V_{Nernst} =$ 44.8 mV calculated for Na^+ ions, which clearly shows that the large anionic polymer cannot permeate through OmpF. In Table 2, calculated permeability ratios obtained under bi-ionic conditions are listed for the three ß-lactamase inhibitors and sodium chloride.

OmpF *Escherichia coli* (DB EGT69961.1)	**ß lactamase inhibitor**	$\boldsymbol{P_{anion^-}/P_{Na^+}}$
	Avibactam-Na	0.32
	Sulbactam-Na	0.25
	Tazobactam-Na	0.28
	NaCl	0.25

Table 2: Bi-ionic permeability ratios of the ß-lactamase inhibitors (P_{anion^-}/P_{Na^+}) for the current flux through OmpF.

If we accept the GHK assumptions, i.e. cations, and anions move independently through the channel, we can use single pore conductance and the obtained relative permeability ratio

P_{anion^-}/P_{Na^+} to separate the individual contributions of cations and anions to the total current determined in a single experiment.[14-17] Using the measured $\bar{G}_{monomer} \cong 90$ pS for avibactam-Na (Table1) at 30 mM (cis/trans) and the selectivity of $P_{avibactam^-}/P_{Na^+} = 0.32$ we calculated the contribution of the anionic avibactam to the total current at V_m = 100 mV using equation (2) at the given concentration gradient of $\Delta c_{cis/trans} = 50\ mM$ (Figure S3). With this, the turnover number of avibactam could be estimated. As reported in Supplemental Information in detail, by extrapolating to low 10µM concentrations we obtained a turnover rate of $n \cong 624$ molecules$/s$ (per trimer) at a concentration gradient of Δc = 10 µM and at zero membrane potential. To investigate the robustness of our approach we also tested the permeability of sulbactam-Na and tazobactam-Na through the OmpF pore under tri-ionic conditions (see Supplemental Information for details). The measured V_{rev} and permeability ratios calculated as described in the Supplemental Information are listed in Table 3.

ß lactamase inhibitor*	NaCl [mM] (cis/trans)	Inhibitor [mM] (cis)	V_{rev} [mV] (exp)	$P_{Na^+}/P_{Cl^-}/P_{inh^-}$ *(calc)***
Sulbactam-Na	10	50	21±6	4:1:1.2
	100	50	5±2	4:1:2.2
Tazobactam-Na	10	50	20±4	4:1:2.2

Table 3: Permeability of Sulbactam-Na and Tazobactam-Na through the OmpF pore under tri-ionic conditions. ** The permeability ratio of $P_{Na^+}/P_{Cl^-} = 4:1$ for OmpF has been determined independently under bionic conditions and was fixed during fitting of V_{rev} (tri-ionic).

The permeability ratio for Na-sulbactam under bionic condition (Table 2) was $P_{SB^-}/P_{Na^+} = 0.25$, which compares with the tri-ionic values of $P_{SB^-}/P_{Na^+} = 0.3$ (10 mM NaCl background) and $P_{SB^-}/P_{Na^+} = 0.55$ (100 mM NaCl background). While the permeability ratio for Na-tazobactam under bionic condition (Table 2) was $P_{TB^-}/P_{Na^+} = 0.28$, which compares with the tri-ionic value P_{TB^-}/P_{Na^+} = 0.45 (at 30 mM Na Cl background).

The significant differences obtained between permeability ratios at different symmetrical NaCl concentrations show that GHK theory assumption of completely independent ion movements through the channel are particularly at higher NaCl background concentrations not met. Nevertheless, the parameters obtained under bi-ionic and tri-ionic conditions with lower NaCl concentrations are within a reasonable range and show that our experimental approach combined with the macroscopic GHK theory can be applied to gain unambiguous information on the fluxes of the ß lactam inhibitors through different porins, otherwise hard to measure directly.

To understand the rapid permeation of the inhibitors at the atomic level, we performed all-atom MD simulations of inhibitors with 200 mM of KCl. The permeation of inhibitors through OmpF was simulated by using well-tempered metadynamics with multiple walkers to accelerate their evolution. On the other hand, the permeation of ions was simulated with unbiased MD simulations and with an external and constant electric field of 200 mV. The reconstructed free energies surfaces (FES) with respect to the axis of diffusion Z showed for inhibitors a central barrier between 3 and 5 kcal/mol, at the constriction region (Figure 2), to be compared with 2 kcal/mol for chloride and less than 1 kcal/mol for potassium. A preferred interaction in the region above the constriction region, the pre-orientation region between 3 and 8 Å from the center, was found, where inhibitors aligned its dipole to the transversal electric field[18-19] and, at the same time, established a direct interaction with the residues of the basic ladder (R167, R168, R82) by its sulfate or carboxylic group.

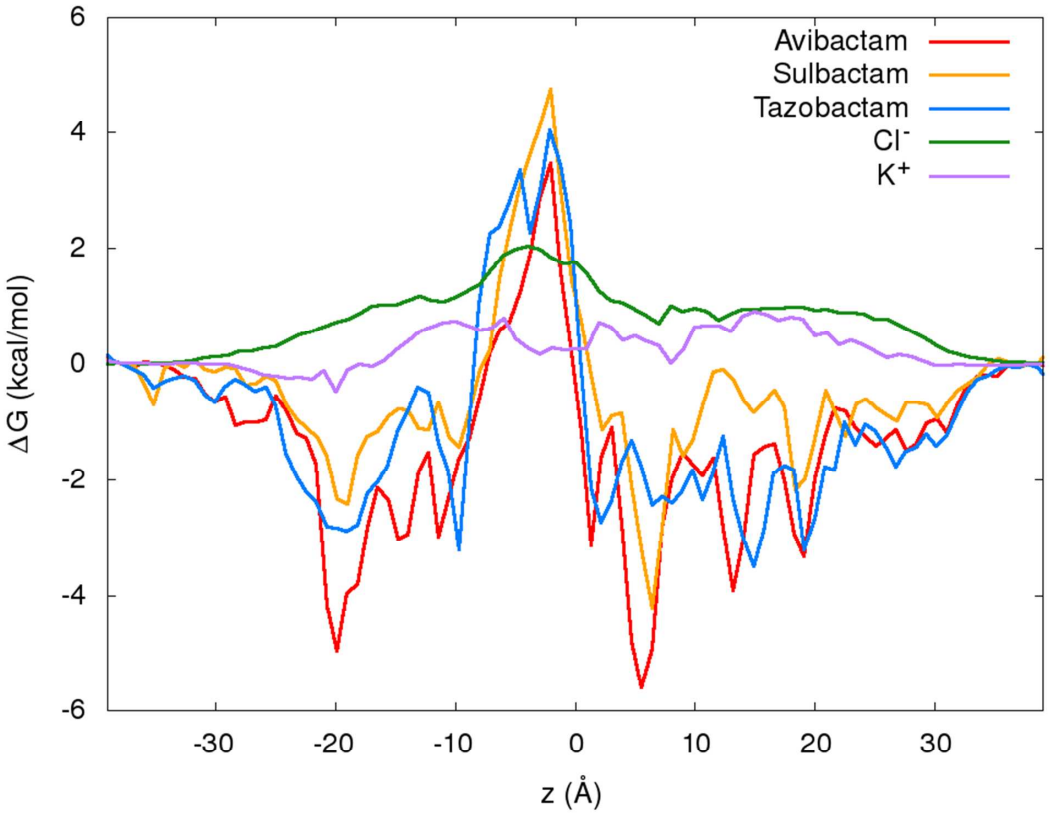

Figure 2: FES reconstructed with metadynamics simulation for the three inhibitors through OmpF, by using two collective variables, namely, molecular dipole orientation and z-coordinate (position along the channel axis). We showed the FES only along the Z coordinate for a comparison with the free energy of ions, calculated with their relative density with respect to the bulk, 200 mM.

Independent 100 ns standard MD simulations were performed at an applied membrane potential of V_m= 200 mV with avibactam only starting from the pre-orientation minimum. Five independent trajectories showed that avibactam stayed in the pre-orientation region when a positive voltage was applied, probably pushed by the external voltage on the one hand, but not able to cross the constriction region barrier on the other, at least in the limited time of 100 ns (Figure S11). In this stable configuration, avibactam occupied the chloride path, while affecting the cations path only to a marginal extent (Figure S12). By calculating the permeability ratio cations/anions, we could highlight an enhanced cation selectivity in the presence of avibactam, probably due to its negative charge coordinating the positive ladder inside the channel, allowing an easier permeation for cations (Table 4). It seems that the decreased anion conductivity, due to avibactam physically occupying anions path (Figure S12), was compensated by the increased cations permeation, Table 4.

The channel conductance can also be estimated using a mean field approach (see Supplemental Information for details). Herein the calculated free energy profiles shown in Figure 2 enter into an effective position-independent diffusion constant $D(x) = D_{eff}$

Ion	***G* [pS]**/mM	**Permeability/P^+**
Diffusion Model with calculated free energies at 200 mM		
K^+	7	1
Cl^-	2.3	0.3
Avibactam(-)	2.2	0.3
Tazobactam(-)	0.6	0.09
Sulbactam(-)	0.25	0.04
MD simulations with external electric field (200 mM and 200 mV, 5 trajectories 100 ns)		
K^+	3.3 ±0.3	1
Cl-	1.1±0.2	0.3
K^+ with one avibactam bound	4.1±0.5	1
Cl^- with one avibactam bound	0.8±0.2	0.2

Table. 4: Comparing conductance obtained from the diffusion model and from standard MD simulations with external electric field applied. Conductance values are normalized to 1 mM. The permeability ratio to the K^+ is shown in the third column. The free energies used as those of Fig. 2.

Discussion

We have shown that recording nanopore I-V curves and fitting the results with the GHK equation gives readily the zero-current potential and thus allows the calculation of the relative permeability for the ions present in solution. In particular, with nanometer sized pores at low mM concentrations of current carrier electrolytes like NaCl the nanopore permeability of large charged solute molecules like the ß lactamase inhibitors anions of avibactam, sulbactam and tazobactam can be screened under tri ionic conditions using low mM to µM concentrations of the charged large solute molecules. Beside the principal difficulties underlying the GHK constant field theory, which assumes independent movement of the ions through the pores (see references [14-16] for a detailed discussion) we have demonstrated that the methodology can be used to obtain semi-quantitative measures for permeation of charged drugs through nanopores. The method presented can, after a suitable miniaturization and parallelization, serve as a basis for a simple, fast and sensitive permeability screen of nanopores for charged molecules. As detailed in the supplemental information for two limiting cases the sensitivity of the method may be estimated: -under bionic conditions, where one of the ions species corresponds to the large molecule in question, a 1.1-fold gradient with down to µM concentration is a realistic lower resolution limit. Using tri-ionic conditions, at 1mM carrier electrolyte, a charged compound concentration of 250 µM (cis or trans) would be sufficient to unambiguously detect whether the large ion is permeant or not.

Further quantification of the flux requires calculation of the individual contribution of each ion species to the total flux passing the single channel. Despite the principal difficulties underlying the GHK constant field theory, using this approach the experimental I-V curves can be divided into the fluxes of the individual ions which then allows a semi-quantitative estimation of turnover numbers of the ions. Comparing our bi ionic and tri ionic measurements and the respective GHK analysis surrounds in a coarse qualitative consistency of the data, which sanctions our conclusions to be qualitatively valid.

Further, using MD-simulations confirmed that in tri-ionic conditions the presence of avibactam inside OmpF has an effect on the selectivity of the channel but rendering the variance of the total conductance within experimental errors (Tab.4).

Surprisingly single channel conductance of the three investigated ß-lactamase is in the same order of magnitude as with NaCl (see Table 1) indicating an unpredictable high permeability. All-atom modeling provides the key to understanding why a large substrate molecule like avibactam, despite having a minimal projection area radius (3.3 Å) close to that of the channel in the constriction region,

diffuses through the channel as fast as the chloride ion having half the size. Inspection of Figure 2 reveals that the free energy of avibactam at the constriction region has a barrier which is nearly double compared to chloride. In contrast, the barrier for the chloride is very broad and extending 50 Å of the channel whereas the barrier for avibactam extends less than 10 Å in the constriction region. The mean field theory as outlined in the supplement reveals readily the correlation between the two parameters of the barrier. The height and the width of the free energy profile impacts the effective diffusion through the integral in Eq. S1.

On a more molecular level the fundamental differences between avibactam and chloride causing the main difference in the free energy profiles is the presence of the dipole moment (~13 D) and the larger size of avibactam. Both reduce the steric barrier all along the channel for avibactam through the desolvation effect and the electrostatic interaction with the internal electric field.[19-20] Generally, our results show that the low uptake of β-lactamase inhibitors observed in many cases by OmpF expressing bacteria cannot be attributed to a low transport capacity of OmpF for these compounds. Rather, additional regulatory processes are likely to control the permeation of the β-lactamase inhibitors through the pore of OmpF presumably at the level of protein-protein interactions.

Associated Contents

Supporting Information: Planar Lipid Bilayer and Electrical Recording, Electrophysiological permeation assay Method-Outline, Calculation of the Avibactam-anion turnover through OmpF, Extended analysis of single channel currents of OmpF in the presence of ß-lactamase-inhibitors, Molecular dynamics calculations, and Methods.

Author Contributions: M.W. and R.W initiated the idea of reversal potential measurements and supervised I.G. in the work. I.G. performed all the experiments and analyzed the data with input from M.W. and R.W. L.B. purified the protein. A.P., M.A.S., I.B., M.C., performed Molecular dynamics calculations. I.G., M.W. R.W, M.C. were involved in the writing of the manuscript.

Acknowledgment: The research leading to these results was conducted as part of the TRANSLOCATION consortium and has received support from the Innovative Medicines Initiatives Joint Undertaking under Grant Agreement n°115525, resources which are composed of financial contribution from the European Union's seventh framework program (FP7/2007-2013) and EFPIA companies in kind contribution.

References:

1. Edel, J.; Oh, S.H., From Nanopores to Nanochannels. *Analyst* 2015, *140*, 4732.
2. Albrecht, T.; Edel, J. B.; Winterhalter, M. New Developments in Nanopore Research--from Fundamentals to Applications. *J. Phys. Condens. Matter* 2010, *22*, 450301.
3. Howorka, S.; Siwy, Z., Nanopore analytics: sensing of single molecules. *Chem.Soc.Rev.* 2009, *38* (8), 2360-2384.
4. Deamer, D.; Akeson, M.; Branton, D., Three decades of nanopore sequencing. *Nat Biotechnol* 2016, *34* (5), 518-524.

5. Hajjar, E.; Mahendran, K. R.; Kumar, A.; Bessonov, A.; Petrescu, M.; Weingart, H.; Ruggerone, P.; Winterhalter, M.; Ceccarelli, M. Bridging Timescales and Length Scales: From Macroscopic Flux to the Molecular Mechanism of Antibiotic Diffusion through Porins. *Biophys. J.* 2010, *98*, 569–575.
6. Nikaido, H., Molecular basis of bacterial outer membrane permeability revisited. *Microbiology and molecular biology reviews* 2003, *67* (4), 593-656.
7. Payne, D. J.; Gwynn, M. N.; Holmes, D. J.; Pompliano, D. L., Drugs for bad bugs: confronting the challenges of antibacterial discovery. *Nature reviews Drug discovery* 2007, *6* (1), 29-40.
8. Stavenger, R. A.; Winterhalter, M., TRANSLOCATION project: how to get good drugs into bad bugs. *Science translational medicine* 2014, *6* (228), 228ed7-228ed.
9. Hille, B., *Ionic Channels of Excitable Membranes*. Sinauer Ass. Inc.: Sunderland, Ma 01375, 2001; Vol. 3.
10. Harsman, A.; Schock, A.; Hemmis, B.; Wahl, V.; Jeshen, I.; Bartsch, P.; Schlereth, A.; Pertl-Obermeyer, H.; Goetze, T. A.; Soll, J., OEP40, a Regulated Glucose-permeable β-Barrel Solute Channel in the Chloroplast Outer Envelope Membrane. *Journal of Biological Chemistry* 2016, *291* (34), 17848-17860.
11. Wagner, R.; Schmedt, D.; Hanhart, P.; Walter, C.; Meisinger, C.; Bartsch, P., Mitochondrial Protein Import Channels. In *Electrophysiology of Unconventional Channels and Pores*, Springer: 2015; pp 33-58.
12. Danelon C, Suenaga A, Winterhalter M, Yamato I. Molecular Origin of the Cation Selectivity in OmpF Porin. Single Channel Conductances versus Free Energy Calculation. Biophys. Chem. 104 (2003) 591.
13. López ML, García-Giménez E, Aguilella VM, Alcaraz A. Critical assessment of OmpF channel selectivity: merging information from different experimental protocols. J Phys Condens Matter. 2010 Nov 17;22(45):454106. doi: 10.1088/0953-8984.
14. Syganow, A.; Von Kitzing, E., (In) validity of the constant field and constant currents assumptions in theories of ion transport. *Biophysical journal* 1999, *76* (2), 768-781.
15. Corry, B.; Kuyucak, S.; Chung, S.-H., Tests of Continuum Theories as Models of Ion Channels. II. Poisson–Nernst–Planck Theory versus Brownian Dynamics. *Biophysical Journal* 2000, *78* (5), 2364-2381.
16. Moy, G.; Corry, B.; Kuyucak, S.; Chung, S.-H., Tests of continuum theories as models of ion channels. I. Poisson− Boltzmann theory versus Brownian dynamics. *Biophysical Journal* 2000, *78* (5), 2349-2363.
17. Chimerel, C.; Movileanu, L.; Pezeshki, S.; Winterhalter, M.; Kleinekathöfer, U. Transport at the nanoscale: Temperature dependence of ion conductance. *European Biophysical Journal* 2000, *838*, 121-5.
18. Acosta-Gutierrez, S.; Scorciapino, M.A.; Bodrenko, I. ; Ceccarelli, M. Filtering with Electric Field: the Case of E. Coli Porins. *Journal of Physical Chemistry Letters* 2015, *6*, 1807-12.
19. Acosta-Gutierrez, S.; Bodrenko, I. ; Scorciapino, M.A.; Ceccarelli, M. Macroscopic Electric Field Inside Water-Filled Biological Nanopores. *Physical Chemistry Chemical Physics* 2016, *18* 8855–64.
20. Malloci, G.; Vargiu, A.; Serra, G.; Bosin A.; Ruggerone, P.; Ceccarelli, M. A Database of Force-Field Parameters, Dynamics, and Properties of Antimicrobial Compounds. *Molecules* 2015, *20*, 13997–4021.
21. Bodrenko, I.; Bajaj, H.; Ruggerone, P.; Winterhalter, M.; Ceccarelli, M., Analysis of fast channel blockage: revealing substrate binding in the microsecond range. *Analyst* **2015,** *140* (14), 4820-4827